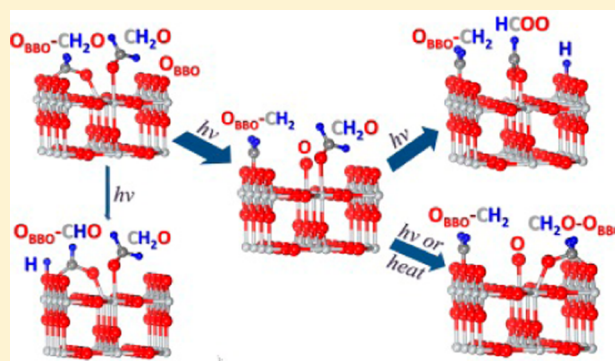


Photoinduced Decomposition of Formaldehyde on a  $\text{TiO}_2(110)$  Surface, Assisted by Bridge-Bonded Oxygen AtomsChenbiao Xu,<sup>†,§</sup> Wenshao Yang,<sup>†</sup> Qing Guo,<sup>\*,†</sup> Dongxu Dai,<sup>†</sup> Timothy K. Minton,<sup>\*,†,‡</sup> and Xueming Yang<sup>\*,†</sup><sup>†</sup>State Key Laboratory of Molecular Reaction Dynamics, Dalian Institute of Chemical Physics, 457 Zhongshan Road, Dalian 116023, Liaoning, P. R. China<sup>‡</sup>Department of Chemistry and Biochemistry, Montana State University, Bozeman, Montana 59717, United States

## Supporting Information

**ABSTRACT:** We have investigated the photoinduced decomposition of formaldehyde ( $\text{CH}_2\text{O}$ ) on  $\text{TiO}_2(110)$  at 400 nm using temperature-programmed desorption. Formate ( $\text{HCOO}$ ), methyl radicals ( $\text{CH}_3$ ), and ethylene ( $\text{C}_2\text{H}_4$ ) have been detected, while no evidence of polymerization of  $\text{CH}_2\text{O}$  was found. The initial step in the decomposition of  $\text{CH}_2\text{O}$  on  $\text{TiO}_2(110)$  is the formation of a dioxymethylene intermediate in which the carbonyl O atom of  $\text{CH}_2\text{O}$  is bound both to a Ti atom on the five-fold-coordinated lattice site ( $\text{Ti}_{5C}$ ) and to a nearby bridge-bonded oxygen (BBO) atom. During 400 nm irradiation, the dioxymethylene intermediate can transfer methylene to the bridging oxygen row and break the C–O bond, thus leaving the original carbonyl O atom on the  $\text{Ti}_{5C}$  site. After this transfer of methylene, several pathways to products are available. Thus we have found that BBO atoms are intimately involved in the photoinduced decomposition of  $\text{CH}_2\text{O}$  on  $\text{TiO}_2(110)$ .

**SECTION:** Surfaces, Interfaces, Porous Materials, and Catalysis



$\text{TiO}_2$  has been investigated as a potential energy-efficient catalyst for photo-oxidation.<sup>1–8</sup> The development of efficient catalysts from  $\text{TiO}_2$  can be facilitated by an understanding of the site-specific surface dynamical processes of adsorbed molecules and reaction intermediates. Much work has been done to study the photocatalysis of organic compounds on  $\text{TiO}_2$ , for example, the degradation of  $\text{CH}_2\text{O}$ <sup>9</sup> and the development of a  $\text{TiO}_2$ -based gas sensor.<sup>10</sup> However, most of the studies are on powders of  $\text{TiO}_2$ .<sup>11–13</sup> To clarify the role of different kinds of active sites and gain a better understanding of photocatalytic reactions, single crystals<sup>14–20</sup> and thin films<sup>12,13</sup> of  $\text{TiO}_2$  have been used as model surfaces for studying photo-oxidation and other photoinduced processes. Among the rutile  $\text{TiO}_2$  surfaces, the (110) single-crystal surface has been especially widely used in fundamental studies of photocatalytic reactions as well as for studies of adsorbate–surface interactions, surface reconstructions, defects, and many other phenomena.

It has been demonstrated that surface  $\text{Ti}^{3+}$  defect sites,<sup>21–24</sup> bulk  $\text{Ti}^{3+}$  defect sites,<sup>25</sup> and surface  $\text{Ti}^{4+}$  sites<sup>26,27</sup> on  $\text{TiO}_2(110)$  play important roles in molecular adsorption, thermal reactions, and photocatalytic reactions. There are also some suggestions in the literature that lattice oxygen plays a role in photo-oxidation reactions on  $\text{TiO}_2$  mainly because of its presence in products or intermediates (as determined through isotopic labeling studies).<sup>28–32</sup> However, a direct mechanistic exper-

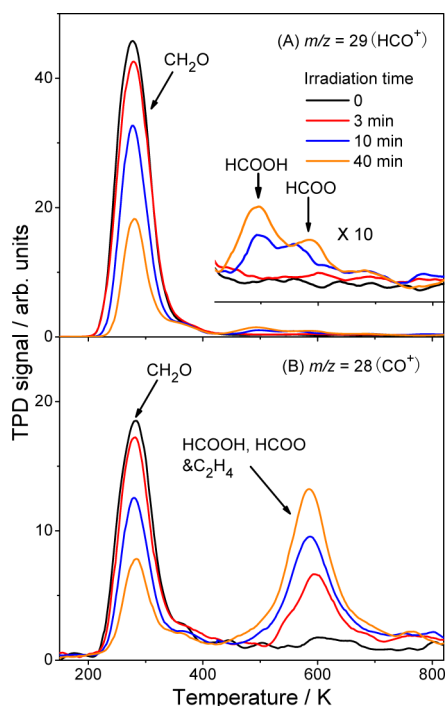
imental study of how lattice oxygen is involved in photochemical reactions on  $\text{TiO}_2$  has not been reported. In this work, we have conducted a temperature-programmed desorption (TPD) investigation of the mechanism of the photoinduced decomposition of  $\text{CH}_2\text{O}$  on a  $\text{TiO}_2(110)$  surface and have identified the important role of the bridge-bonded oxygen (BBO) atoms in the first step toward the final reaction products: formate,  $\text{C}_2\text{H}_4$ , and  $\text{CH}_3$ .

Figure 1 shows TPD spectra collected at mass-to-charge ratios ( $m/z$ ) of 28 ( $\text{CO}^+$ ,  $\text{C}_2\text{H}_4^+$ ) and 29 ( $\text{HCO}^+$ ) after surfaces of  $\text{TiO}_2(110)$  were dosed with 0.55 ML of  $\text{CH}_2\text{O}$  and then irradiated by a laser at 400 nm for various durations. Before irradiation, the signal profile of the 280 K peak from  $m/z = 28$  and 29 was exactly the same as that from  $m/z = 30$  ( $\text{CH}_2\text{O}^+$ ; see in Figure S1 in Supporting Information), suggesting that all of these peaks are the result of dissociative ionization of the desorbed parent  $\text{CH}_2\text{O}$  molecule in the electron-bombardment ionizer. An additional, weak peak with the same shape was collected at  $m/z = 31$ , which is presumably the result of the ions,  $\text{CHDO}^+$  and  $\text{HC}^{18}\text{O}^+$ , that originate from naturally abundant isotopologues of formaldehyde. The respective

Received: June 30, 2013

Accepted: July 26, 2013

Published: July 26, 2013



**Figure 1.** Reduced  $\text{TiO}_2(110)$  was dosed with 0.55 ML of  $\text{CH}_2\text{O}$  at 110 K. (A) Typical TPD spectra collected at  $m/z = 29$  ( $\text{HCO}^+$ ) following different laser irradiation times. (B) Typical TPD spectra collected at  $m/z = 28$  ( $\text{C}_2\text{H}_4^+$ ,  $\text{CO}^+$ ) following different laser irradiation times.

relative intensities at  $m/z = 29$ , 30, and 31 may be compared with tabulated intensities of these ion fragments for the formaldehyde monomer (1, 0.58, and 0.005) and the cyclic formaldehyde trimer, 1,3,5-trioxane (0.26, 0.15, and 1).<sup>33</sup> The observed fragmentation intensity ratios clearly indicate that the desorption is strongly dominated by formaldehyde monomers. The  $\text{CH}_2\text{O}$  peak at 280 K decreases monotonically as the laser irradiation time increases, suggesting that the  $\text{CH}_2\text{O}$  molecules that are adsorbed on the  $\text{Ti}_{5c}$  sites of  $\text{TiO}_2(110)$  either desorb or react to form other products.

A 360 K shoulder becomes obvious in the  $m/z = 29$  TPD spectrum after irradiation (Figure 1A), suggesting the formation of a product that is more strongly bound to the surface than  $\text{CH}_2\text{O}$ . Taking into account additional TPD traces (Figure S1, Supporting Information), the 360 K shoulder is also assigned to  $\text{CH}_2\text{O}$ . Recent theoretical results<sup>34,35</sup> show that a dioxymethylene structure involving  $\text{CH}_2\text{O}$  can form on a  $\text{TiO}_2(110)$  surface, where the carbonyl O atom of  $\text{CH}_2\text{O}$  is bound both to a  $\text{Ti}_{5c}$  site and to an adjacent BBO atom. This structure has an adsorption energy of 1.1 to 1.3 eV, which implies that it is more stable than molecularly adsorbed  $\text{CH}_2\text{O}$  that is bound to the surface solely through an O– $\text{Ti}_{5c}$  bond (0.5 to 0.6 eV). Previous Fourier-transform infrared (FTIR) spectroscopy results of  $\text{CH}_2\text{O}$  adsorption on fully oxidized (defect-free) and reduced (with O-atom vacancies)  $\text{TiO}_2$  surfaces are suggestive of two adsorption modes in which one is an  $\eta^1$  configuration (O adsorption structure) and the other an  $\eta^2$  configuration (C, O adsorption structure).<sup>36–38</sup> High-resolution electron energy loss spectroscopy (HREELS) studies<sup>39</sup> of  $\text{CH}_2\text{O}$  on  $\text{TiO}_2(110)$  clearly observed a C–O stretching vibration in O–C–O units, and the authors attributed this observation to paraformaldehyde formation on the  $\text{TiO}_2(110)$  surface. However, later TPD investigation-

s<sup>40,41</sup> of formaldehyde polymerization on  $\text{TiO}_2(110)$  and on a  $(\text{WO}_3)_3/\text{TiO}_2(110)$  model catalyst found no evidence of paraformaldehyde formation, as the sole desorption of  $\text{CH}_2\text{O}$  monomers was clearly evident on  $\text{TiO}_2(110)$ . This conclusion is similar to that from a previous formaldehyde polymerization study with powders of  $\text{TiO}_2$  and  $(\text{WO}_3)_3/\text{TiO}_2$ .<sup>42</sup> Therefore, we conclude that a dioxymethylene structure involving adsorbed  $\text{CH}_2\text{O}$  on  $\text{TiO}_2(110)$  is the only candidate for the HREELS observation of a C–O stretching vibration in O–C–O units and our observation of the increasing 360 K shoulder after irradiation.

Two additional new desorption features at 486 and 580 K grow in the  $m/z = 29$  TPD spectrum with increasing irradiation times. TPD traces were collected at a variety of  $m/z$  ratios to assign the new features (Figure S1 in Supporting Information). Compared with previous studies of  $\text{HCOOH}$  adsorbed on  $\text{TiO}_2(110)$ <sup>43</sup> and the cracking pattern of  $\text{HCOOH}$  observed in our mass spectrometer (see Figure S2 in Supporting Information), the 486 K peak here is assigned to the recombination of surface formates with surface hydroxyl groups at BBO sites, and the 580 K peak at  $m/z = 29$  is assigned to the desorption of formates and, possibly, of a secondary  $\text{CH}_2\text{O}$  product from the decomposition of formates.

Concomitant to the decrease in the  $\text{CH}_2\text{O}$  TPD peak, the TPD signal for  $m/z = 28$  at 580 K increases with increasing laser irradiation times (Figure 1B). The  $m/z = 28$  signal at 580 K may come from three sources. The first is an ethylene ( $\text{C}_2\text{H}_4$ ) product that arises from  $\text{CH}_2\text{O}$  adsorbed on oxygen defect sites to form a diolate ( $-\text{OCH}_2\text{CH}_2\text{O}-$ ) species, which releases  $\text{C}_2\text{H}_4$  at a relatively high TPD temperature near 620 K.<sup>21,39</sup> Taking into account correction factors for mass spectrometer sensitivity and assuming all of the signal in the  $m/z = 28$  TPD peak comes from  $\text{C}_2\text{H}_4$  before irradiation, the ratio of  $\text{C}_2\text{H}_4$ -to- $\text{CH}_2\text{O}$  product desorption is found to be 4%, which is consistent with an oxygen defect concentration of  $\sim 4\%$ , as indicated by the TPD of water.<sup>44</sup> As indicated in Figure 1B, the other two sources of  $m/z = 28$  signal at 580 K are  $\text{HCOOH}$  and formate, both of which could be photo-oxidation products. In previous investigations of  $\text{HCOOH}$  adsorbed on  $\text{TiO}_2(110)$ ,<sup>40,45–47</sup> the main species on the surface is formate when the surface temperature is higher than 500 K. Therefore, CO is observed to desorb at 580 K as a result of the decomposition of the formate species.

The large TPD signal for desorbed CO seen in Figure 1B indicates that formate is an important photoinduced product. Compared with other products, the 580 K peak intensity is  $>10$  times greater (see Figure S1 in Supporting Information), strongly suggesting that formate is the main product of the photoinduced decomposition of  $\text{CH}_2\text{O}$  on  $\text{TiO}_2(110)$ . The yields of CO (from formate) and  $\text{CH}_2\text{O}$  with irradiation time are shown in Figure 2. About 0.35 ML of  $\text{CH}_2\text{O}$  was depleted during 40 min of irradiation, whereas only 0.08 ML of formate was produced, implying that the decrease in the  $\text{CH}_2\text{O}$  signal is mainly the result of desorption of  $\text{CH}_2\text{O}$  during laser irradiation. Indeed, a large photoinduced desorption signal of  $\text{CH}_2\text{O}$  at  $m/z = 30$  was observed during irradiation by a time-of-flight (TOF) method (see Figure S3 in Supporting Information), implying that a significant fraction of  $\text{CH}_2\text{O}$  is desorbed during irradiation.

To produce formate, the carbon atom of the reagent  $\text{CH}_2\text{O}$  molecule must acquire a second O atom. Previous studies of acetone and acetaldehyde photochemistry on preoxidized  $\text{TiO}_2(110)$ <sup>18,19,48–51</sup> demonstrate that acetone or acetaldehyde

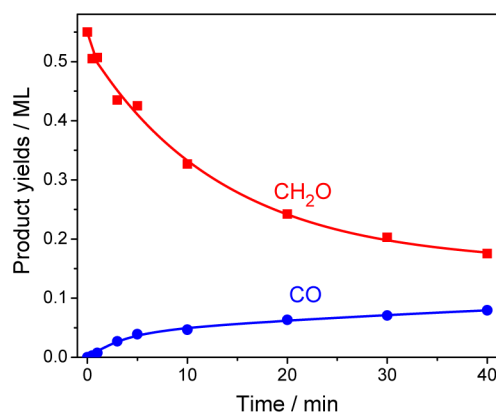


**Figure 2.** Yields of CH<sub>2</sub>O and CO (from formate) as a function of irradiation time following adsorption of 0.55 ML of CH<sub>2</sub>O on a TiO<sub>2</sub>(110) surface at 110 K, derived from data in Figure 1. The contribution of C<sub>2</sub>H<sub>4</sub> has been subtracted.

adsorbed on preoxidized TiO<sub>2</sub>(110) undergoes a facile thermal reaction to form a photoactive acetone–oxygen or acetaldehyde–oxygen complex first; then, UV irradiation of the acetone–oxygen or acetaldehyde–oxygen complex results in the ejection of a methyl radical into gas phase and conversion of the surface-bound fragment into acetate or formate. Formate was also observed as the main product in our experiments, even without preoxidation of the surface, implying that CH<sub>2</sub>O acquires an additional O atom either from a BBO row or from another CH<sub>2</sub>O molecule adsorbed on the surface. A series of studies<sup>40–42</sup> show that polymerization of formaldehyde cannot be achieved by heat on pure TiO<sub>2</sub>. In our experiments, the lack of TPD signals at  $m/z > 30$  show that paraformaldehyde is not produced during UV irradiation (not shown), implying that HCOOH formation from direct reaction of two CH<sub>2</sub>O molecules is also unlikely. The direct photodissociation of CH<sub>2</sub>O to produce an O atom via C=O bond breakage is also not possible because of the low adsorption cross section of CH<sub>2</sub>O at 400 nm ( $\sim 10^{-23}$  cm<sup>2</sup>).<sup>52</sup> Therefore, the most likely reaction must involve the transfer of methylene from CH<sub>2</sub>O to a BBO atom during UV irradiation through an intermediate adsorption structure consisting of dioxymethylene, with the O atom of CH<sub>2</sub>O remaining on a Ti<sub>5C</sub> site. The O atom may react with a nearby adsorbed CH<sub>2</sub>O molecule to form a CH<sub>2</sub>O–O complex; then, formate can be produced by the transfer of an H atom to a BBO site or the ejection of the H atom into the vacuum. As shown in Figure 1A, the increasing signal intensity for recombinative desorption of HCOOH from H atoms on BBO rows and formates strongly suggests that H atoms are transferred to BBO sites from the CH<sub>2</sub>O–O complex during UV irradiation. In addition, the increasing signal intensity for the recombinative desorption of H<sub>2</sub>O from hydroxyls on BBO rows (see Figure S4 in Supporting Information) also verifies this reaction channel. The high background at  $m/z = 1$  in the mass spectrometer made it impossible to observe an H-atom TOF signal and verify the possibility of H-atom ejection into the vacuum.

The conclusion of a dioxymethylene intermediate is supported by the observation of other products. Typical TPD spectra for  $m/z = 26$  (C<sub>2</sub>H<sub>2</sub><sup>+</sup>) are shown in Figure 3A. As reported in previous studies,<sup>21,39</sup> the 620 K peak at  $m/z = 26$  comes from C<sub>2</sub>H<sub>4</sub>, which is produced by the carbon–carbon bond formation reaction of two CH<sub>2</sub>O molecules adsorbed on vacancy sites. A TPD spectrum at  $m/z = 27$  verifies that the  $m/z$

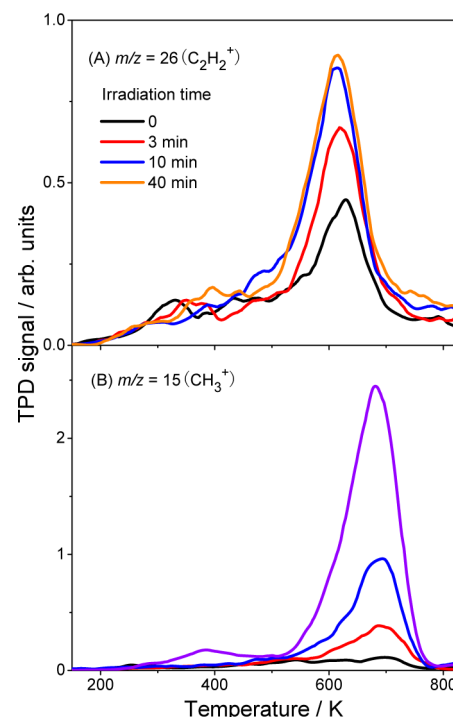


**Figure 3.** Reduced TiO<sub>2</sub>(110) was dosed with 0.55 ML of CH<sub>2</sub>O at 110 K. (A) Typical TPD spectra collected at  $m/z = 26$  (C<sub>2</sub>H<sub>2</sub><sup>+</sup>) following different laser irradiation times. (B) Typical TPD spectra collected at  $m/z = 15$  (CH<sub>3</sub><sup>+</sup>) following different laser irradiation times.

$z = 26$  signal is from the fragmentation of C<sub>2</sub>H<sub>4</sub>. (See Figure S1 in the Supporting Information.) The increase in the C<sub>2</sub>H<sub>4</sub> signal with irradiation time is strong evidence that methylene groups are transferred to BBO atoms as a result of UV irradiation.

Another broad peak appears at 680 K in the TPD spectrum at  $m/z = 15$  (CH<sub>3</sub><sup>+</sup>) after irradiation and increases with irradiation time. This peak is attributed to CH<sub>3</sub> desorption from BBO atoms, consistent with our previous studies.<sup>27</sup> A separate experiment with CH<sub>3</sub>OH-covered TiO<sub>2</sub>(110) was carried out to confirm methyl radical desorption. (See Figure S5 in Supporting Information.) However, the desorption temperature of CH<sub>3</sub> on BBO sites is 30 K higher than that observed in previous studies,<sup>27</sup> which may be due to a temperature measurement offset. The appearance and increase of CH<sub>3</sub> products on BBO atoms after UV irradiation further demonstrates that methylene groups can be transferred to bridging oxygen during irradiation. These methylene groups may form CH<sub>3</sub> by reacting with H atoms on BBO sites. The CH<sub>3</sub> products would adsorb on BBO sites more strongly than methylene. The yields of CH<sub>3</sub> and C<sub>2</sub>H<sub>4</sub> following 0.55 ML adsorption of CH<sub>2</sub>O on TiO<sub>2</sub>(110) are shown in Figure 4. The yield of C<sub>2</sub>H<sub>4</sub> increases very fast to reach a plateau, while the yield of CH<sub>3</sub> continues to increase. After 40 min of irradiation, the total amount of methylene that has transferred to bridging oxygen is  $\sim 0.06$  ML,  $\sim 0.02$  ML less than the amount of formate that has been formed.

A schematic model for the photoinduced decomposition of CH<sub>2</sub>O is depicted in Figure 5. First, two adsorption structures of CH<sub>2</sub>O (CH<sub>2</sub>O molecularly adsorbed to a surface Ti<sub>5C</sub> atom solely through an O–Ti<sub>5C</sub> bond and CH<sub>2</sub>O molecularly adsorbed to the rutile (110) surface through O–Ti<sub>5C</sub> and C–



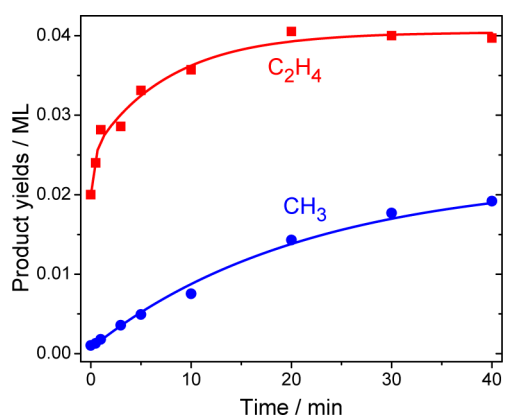


**Figure 4.** Yields of C<sub>2</sub>H<sub>4</sub> and CH<sub>3</sub> as a function of irradiation time following adsorption of 0.55 ML of CH<sub>2</sub>O on a TiO<sub>2</sub>(110) surface at 110 K, derived from data in Figure 3.

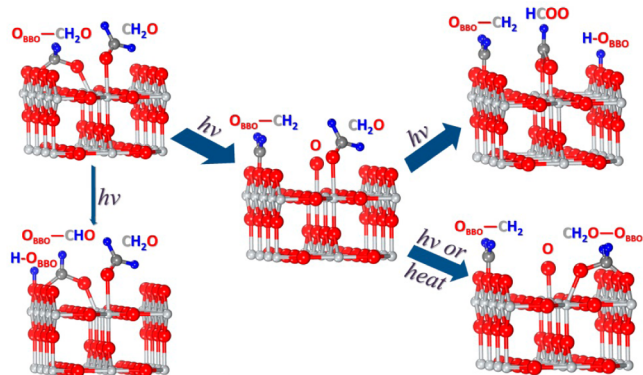


**Figure 5.** Schematic model for bridging-oxygen-assisted, photoinduced decomposition of CH<sub>2</sub>O on reduced TiO<sub>2</sub>(110).

O<sub>2</sub>C (two-fold coordinated bridging oxygen) bonds exist after exposure of 0.55 ML CH<sub>2</sub>O to the TiO<sub>2</sub>(110) surface. Then, the methylene of CH<sub>2</sub>O may transfer from the dioxymethylene structure to a BBO atom through a photoinduced process, with the O atom of CH<sub>2</sub>O remaining on a Ti<sub>5</sub>C site. This O atom may react with a nearby CH<sub>2</sub>O to form a CH<sub>2</sub>O–O complex by heat or photon irradiation. Eventually, formate is produced when an H atom transfers to a BBO site from the CH<sub>2</sub>O–O complex. This is the main reaction channel for formate production. The formation of the C<sub>2</sub>H<sub>4</sub> and CH<sub>3</sub> products occurs through reactions of the methylene on the BBO rows. As previously mentioned, the amount of formate is larger than the amount of methylene that transferred to BBO sites, which suggests that another form of formate may exist. Previous STM studies of HCOOH on a TiO<sub>2</sub>(110) surface<sup>46,47</sup> do show two kinds of formates. One type of formate adsorbs on the TiO<sub>2</sub>(110) surface through two O–Ti<sub>5</sub>C bonds, and the other type adsorbs through C–O–Ti<sub>5</sub>C and C–O<sub>2</sub>C bonds with the original C–O bond of carbonyl along the [110] orientation on the rutile (110) surface. In the case of CH<sub>2</sub>O adsorption, this adsorption structure is formed by transferring an H atom from dioxymethylene to a BBO site.

Our TPD investigation demonstrates that BBO atoms play a very important role in the photoinduced decomposition of CH<sub>2</sub>O on TiO<sub>2</sub>(110) through an initial dioxymethylene intermediate structure. Formate (of two types) is the most important product, but C<sub>2</sub>H<sub>4</sub> and CH<sub>3</sub> are also significant. Clear mechanisms have been delineated for the participation of

lattice (BBO) atoms in four decomposition pathways, including their presence in one type of formate product.

## EXPERIMENTAL METHODS

TPD experiments were carried out in an ultrahigh vacuum (UHV) chamber with a base pressure of  $6 \times 10^{-11}$  Torr. Details of the TPD apparatus have been described elsewhere.<sup>27</sup> A quadrupole mass spectrometer (Extrel) was used to detect desorbing products. An extremely high vacuum of  $1.5 \times 10^{-12}$  Torr in the electron-impact ionization region was achieved and maintained during the experiment. The rutile TiO<sub>2</sub>(110) crystal, obtained from Princeton Scientific and having dimensions of  $10 \times 10 \times 1.0$  mm<sup>3</sup>, was mounted on a Ta metal plate attached to a liquid-nitrogen-cooled sample holder for cooling to  $\sim 100$  K and resistive heating to  $>900$  K. The surface was cleaned by cycles of Ar<sup>+</sup> sputtering and UHV annealing until common impurities on TiO<sub>2</sub>, such as Ca, K, and C, were not detected by Auger electron spectroscopy (AES), and a sharp  $(1 \times 1)$  low-energy electron diffraction (LEED) pattern was observed. After this preparation procedure, the crystal color became blue and an oxygen vacancy population of 4% remained, as gauged by water TPD.<sup>44</sup> Daily cleaning was accomplished by annealing the crystal at 850 K for 30 min in UHV. At room temperature, the vapor pressure of CH<sub>2</sub>O produced from paraformaldehyde (95% purity, Sigma-Aldrich) was high enough for our experiments. The surface was dosed with 0.55 ML (1 ML =  $5.2 \times 10^{14}$  molecules cm<sup>-2</sup>) coverage of CH<sub>2</sub>O using a home-built, calibrated molecular beam doser at 110 K. The surface temperature typically rose to  $\sim 130$  K during subsequent irradiation. The irradiating laser light had a nominal wavelength of 400 nm, a pulse width of  $\sim 50$  fs, and a bandwidth of  $\sim 20$  nm (second-harmonic of Ti/sapphire laser, Legend Elite, Coherent, 1 kHz). The average power of the light was 150 mW, corresponding to  $\sim 5.4 \times 10^{17}$  photons cm<sup>-2</sup> s<sup>-1</sup>. A previous study in our lab implies that multiphoton effects are not important at this photon flux.<sup>53</sup> The laser irradiation area on the surface was the elliptical projection of a 6 mm diameter laser beam with an angle of  $\sim 30^\circ$  between the surface parallel and laser direction. The TiO<sub>2</sub>(110) surface was annealed in vacuum at 850 K for 20 min between TPD experiments to flatten and clean the surface. TPD signals were collected after irradiation with a heating rate of 2 K/s and with the sample facing the mass spectrometer detector.

## ASSOCIATED CONTENT

### Supporting Information

TPD spectra acquired at a variety of different mass-to-charge ratios after a CH<sub>2</sub>O-adsorbed TiO<sub>2</sub>(110) surface was irradiated by UV light. TPD spectra acquired at a variety of different mass-to-charge ratios after HCOOH was adsorbed on a TiO<sub>2</sub>(110) surface. Time-of-flight signal of CH<sub>2</sub>O ejected during UV irradiation. TPD spectra of H<sub>2</sub>O after a CH<sub>2</sub>O-adsorbed TiO<sub>2</sub>(110) surface was irradiated by UV light. TPD spectra of CH<sub>3</sub> after a CH<sub>3</sub>OH-adsorbed TiO<sub>2</sub>(110) surface was irradiated by UV light. This material is available free of charge via the Internet at <http://pubs.acs.org>.

## AUTHOR INFORMATION

### Corresponding Author

\*E-mail: guoqing@dicp.ac.cn (G.Q.), tminton@montana.edu (T.K.M.), xmyang@dicp.ac.cn (X.Y.).

## Present Address

<sup>§</sup>Chenbiao Xu: Also with School of Physics and Optoelectric Engineering, Dalian University of Technology, Dalian, Liaoning 116023, China.

## Notes

The authors declare no competing financial interest.

## ACKNOWLEDGMENTS

This work was supported by the Chinese Academy of Sciences, National Science Foundation of China, and the Chinese Ministry of Science and Technology.

## REFERENCES

- (1) Hoffmann, M. R.; Martin, S. T.; Choi, W. Y.; Bahnemann, D. W. Environmental Applications of Semiconductor Photocatalysis. *Chem. Rev.* **1995**, *95*, 69–96.
- (2) Thompson, T. L.; Yates, J. T., Jr. Surface Science Studies of the Photoactivation of TiO<sub>2</sub> New Photochemical Processes. *Chem. Rev.* **2006**, *106*, 4428–4453.
- (3) Henderson, M. A.; Otero-Tapia, S.; Castro, M. E. The Chemistry of Methanol on the TiO<sub>2</sub>(110) Surface: the Influence of Vacancies and Coadsorbed Species. *Faraday Discuss.* **1999**, *114*, 313–319.
- (4) Gong, X.-Q.; Selloni, A.; Dulub, O.; Jacobson, P.; Diebold, U. Small Au and Pt Clusters at the Anatase TiO<sub>2</sub>(101) Surface: Behavior at Terraces, Steps, and Surface Oxygen Vacancies. *J. Am. Chem. Soc.* **2008**, *130*, 370–381.
- (5) Henderson, M. A. A Surface Science Perspective on TiO<sub>2</sub> Photocatalysis. *Surf. Sci. Rep.* **2011**, *66*, 185–297.
- (6) Pang, C. L.; Lindsay, R.; Thornton, G. Chemical Reactions on Rutile TiO<sub>2</sub>(110). *Chem. Soc. Rev.* **2008**, *37*, 2328–2353.
- (7) Fujishima, A.; Zhang, X.; Tryk, D. TiO<sub>2</sub> Photocatalysis and Related Surface Phenomena. *Surf. Sci. Rep.* **2008**, *63*, 515–582.
- (8) Diebold, U. The Surface Science of Titanium Dioxide. *Surf. Sci. Rep.* **2003**, *48*, 53–229.
- (9) Zang, L.; Lange, C.; Abraham, I.; Storck, S.; Maier, W. F.; Kisch, H. Amorphous Microporous Titania Modified with Platinum(IV) Chloride-A New Type of Hybrid Photocatalyst for Visible Light Detoxification. *J. Phys. Chem. B* **1998**, *102*, 10765–10771.
- (10) Yanga, L.; Liu, Z.; Shia, J.; Zhanga, Y.; Hua, H.; Shangguan, W. Degradation of Indoor Gaseous Formaldehyde by Hybrid VUV and TiO<sub>2</sub>/UV Processes. *Sep. Purif. Technol.* **2007**, *54*, 204–211.
- (11) Yang, Y. Z.; Chang, C.-H.; Idriss, H. Photo-Catalytic Production of Hydrogen from Ethanol over M/TiO<sub>2</sub> Catalysts (M = Pd, Pt or Rh). *Appl. Catal., B* **2006**, *67*, 217–222.
- (12) Chang, Z.; Thornton, G. Reactivity of Thin-Film TiO<sub>2</sub>(110). *Surf. Sci.* **2000**, *462*, 68–76.
- (13) Herman, G. S.; Gao, Y.; Tran, T. T.; Osterwalder, J. X-ray Photoelectron Diffraction Study of an Anatase Thin Film: TiO<sub>2</sub>(001). *Surf. Sci.* **2000**, *447*, 201–211.
- (14) White, J. M.; Henderson, M. A. Trimethyl Acetate on TiO<sub>2</sub>(110): Preparation and Anaerobic Photolysis. *J. Phys. Chem. B* **2005**, *109*, 12417–12430.
- (15) White, J. M.; Szanyi, J.; Henderson, M. A. Thermal Chemistry of Trimethyl Acetic Acid on TiO<sub>2</sub>(110). *J. Phys. Chem. B* **2004**, *108*, 3592–3602.
- (16) Jayaweera, P. M.; Quah, E. L.; Idriss, H. Photoreaction of Ethanol on TiO<sub>2</sub>(110) Single-Crystal Surface. *J. Phys. Chem. C* **2007**, *111*, 1764–1769.
- (17) Henderson, M. A. Acetone and Water on TiO<sub>2</sub> (110): Competition for Sites. *Langmuir* **2005**, *21*, 3443–3450.
- (18) Henderson, M. A. Relationship of O<sub>2</sub> Photodesorption in Photooxidation of Acetone on TiO<sub>2</sub>. *J. Phys. Chem. C* **2008**, *112*, 11433–14440.
- (19) Henderson, M. A. Photooxidation of Acetone on TiO<sub>2</sub>(110): Conversion to Acetate via Methyl Radical Ejection. *J. Phys. Chem. B* **2005**, *109*, 12062–12070.
- (20) Zehr, R. T.; Henderson, M. A. Acetaldehyde Photochemistry on TiO<sub>2</sub>(110). *Surf. Sci.* **2008**, *602*, 2238–2249.
- (21) Lu, G.; Linsebigler, A.; Yates, J. T., Jr. Ti<sup>3+</sup> Defect Sites on TiO<sub>2</sub>(110): Production and Chemical Detection of Active Sites. *J. Phys. Chem.* **1994**, *98*, 11733–11738.
- (22) Farfan-Arribas, E.; Madix, R. J. Role of Defects in the Adsorption of Aliphatic Alcohols on the TiO<sub>2</sub>(110) Surface. *J. Phys. Chem. B* **2002**, *106*, 10680–10692.
- (23) Henderson, M. A.; Szanyi, J.; Peden, C. H. F. Conversion of N<sub>2</sub>O to N<sub>2</sub> on TiO<sub>2</sub> (110). *Catal. Today* **2003**, *85*, 251–266.
- (24) Lisachenko, A. A.; Mikhailov, R. V.; Basov, L. L.; Shelimov, B. N.; Che, M. Photocatalytic Reduction of NO by CO on Titanium Dioxide under Visible Light Irradiation. *J. Phys. Chem. C* **2007**, *111*, 14440–14447.
- (25) Lira, E.; Wendt, S.; Huo, P.; Hansen, J. Ø.; Sreber, R.; Porsgaard, S.; Wei, Y.; Bechstein, R.; Lægsgaard, E.; Besenbacher, F. The Importance of Bulk Ti<sup>3+</sup> Defects in the Oxygen Chemistry on Titania Surfaces. *J. Am. Chem. Soc.* **2011**, *133*, 6529–6532.
- (26) Zhou, C.; Ren, Z.; Tan, S.; Ma, Z.; Mao, X.; Dai, D.; Fan, H.; Yang, X.; LaRue, J.; Cooper, R.; et al. Site-Specific Photocatalytic Splitting of Methanol on TiO<sub>2</sub>(110). *Chem. Sci.* **2010**, *1*, 575–580.
- (27) Guo, Q.; Xu, C.; Ren, Z.; Yang, W.; Ma, Z.; Dai, D.; Fan, H.; Minton, T. K.; Yang, X. Stepwise Photocatalytic Dissociation of Methanol and Water on TiO<sub>2</sub>(110). *J. Am. Chem. Soc.* **2012**, *134*, 13366–13373.
- (28) Zhuang, J.; Rusu, C. N.; Yates, J. T., Jr. Adsorption and Photooxidation of CH<sub>3</sub>CN on TiO<sub>2</sub>. *J. Phys. Chem. B* **1999**, *103*, 6957–6967.
- (29) Muggli, D. S.; Falconer, J. L. Role of Lattice Oxygen in Photocatalytic Oxidation on TiO<sub>2</sub>. *J. Catal.* **2000**, *191*, 318–325.
- (30) Blount, M. C.; Buchholz, J. A.; Falconer, J. L. Photocatalytic Decomposition of Aliphatic Alcohols, Acids, and Esters. *J. Catal.* **2001**, *197*, 303–314.
- (31) Lee, G. D.; Falconer, J. L. Transient Measurements of Lattice Oxygen in Photocatalytic Decomposition of Formic Acid on TiO<sub>2</sub>. *Catal. Lett.* **2000**, *70*, 145–148.
- (32) Thompson, T. L.; Panayotov, D. A.; Yates, J. T., Jr.; Martynov, I.; Klabunde, K. Photodecomposition of Adsorbed 2-Chloroethyl Ethyl Sulfide on TiO<sub>2</sub>: Involvement of Lattice Oxygen. *J. Phys. Chem. B* **2004**, *108*, 17857–17865.
- (33) NIST Chemistry WebBook, webbook.nist.gov/chemistry.
- (34) Haubrich, J.; Kaxiras, E.; Friend, C. M. The Role of Surface and Subsurface Point Defects for Chemical Model Studies on TiO<sub>2</sub>: A First-Principles Theoretical Study of Formaldehyde Bonding on Rutile TiO<sub>2</sub>(110). *Chem.—Eur. J.* **2011**, *17*, 4496–4506.
- (35) Liu, H.; Wang, X.; Pan, C.; Liew, K. M. First-Principles Study of Formaldehyde Adsorption on TiO<sub>2</sub> Rutile (110) and Anatase (001) Surfaces. *J. Phys. Chem. C* **2012**, *116*, 8044–8053.
- (36) Busca, G.; Lamotte, J.; Lavalley, J.-C.; Lorenzelli, V. FT-IR Study of the Adsorption and Transformation of Formaldehyde on Oxide Surfaces. *J. Am. Chem. Soc.* **1987**, *109*, 5197–5202.
- (37) Kecskés, T.; Raskó, J.; Kiss, J. FTIR and Mass Spectrometric Study of HCOOH Interaction with TiO<sub>2</sub> Supported Rh and Au Catalysts. *Appl. Catal., A* **2004**, *268*, 9–16.
- (38) Raskó, J.; Kecskés, T.; Kiss, J. Adsorption and Reaction of Formaldehyde on TiO<sub>2</sub>-Supported Rh Catalysts Studied by FTIR and Mass Spectrometry. *J. Catal.* **2004**, *226*, 183–191.
- (39) Qiu, H.; Idriss, H.; Wang, Y.; Wöll, C. Carbon–Carbon Bond Formation on Model Titanium Oxide Surfaces: Identification of Surface Reaction Intermediates by High-Resolution Electron Energy Loss Spectroscopy. *J. Phys. Chem. C* **2008**, *112*, 9828–9834.
- (40) Kim, J.; Kay, B. D.; Dohnálek, Z. Formaldehyde Polymerization on (WO<sub>3</sub>)<sub>3</sub>/TiO<sub>2</sub>(110) Model Catalyst. *J. Phys. Chem. C* **2010**, *114*, 17017–17022.
- (41) Valentin, C. D.; Rosa, M.; Pacchioni, G. Radical versus Nucleophilic Mechanism of Formaldehyde Polymerization Catalyzed by (WO<sub>3</sub>)<sub>3</sub> Clusters on Reduced or Stoichiometric TiO<sub>2</sub>(110). *J. Am. Chem. Soc.* **2012**, *134*, 14086–14098.

- (42) Chakraborty, A. K.; Chai, S. Y.; Lee, W. I. Photocatalytic Behavior of  $\text{WO}_3/\text{TiO}_2$  in Decomposing Volatile Aldehydes. *Bull. Korean Chem. Soc.* **2008**, *29*, 494–496.
- (43) Henderson, M. A. Complexity in the Decomposition of Formic Acid on the  $\text{TiO}_2(110)$  Surface. *J. Phys. Chem. B* **1997**, *101*, 221–229.
- (44) Zehr, R. T.; Henderson, M. A. Influence of  $\text{O}_2$ -Induced Surface Roughening on the Chemistry of Water on  $\text{TiO}_2(110)$ . *Surf. Sci.* **2008**, *602*, 1507–1516.
- (45) Bowker, M.; Stone, P.; Bennett, R.; Perkins, N. Formic Acid Adsorption and Decomposition on  $\text{TiO}_2(110)$  and on  $\text{Pd}/\text{TiO}_2(110)$  Model Catalysts. *Surf. Sci.* **2002**, *511*, 435–448.
- (46) Sayago, D. I.; Polcik, M.; Lindsay, R.; Toomes, R. L.; Hoeft, J. T.; Kittel, M.; Woodruff, D. P. Structure Determination of Formic Acid Reaction Products on  $\text{TiO}_2(110)$ . *J. Phys. Chem. B* **2004**, *108*, 14316–14323.
- (47) Aizawa, M.; Morikawa, Y.; Namai, Y.; Morikawa, H.; Iwasawa, Y. Oxygen Vacancy Promoting Catalytic Dehydration of Formic Acid on  $\text{TiO}_2(110)$  by In Situ Scanning Tunneling Microscopic Observation. *J. Phys. Chem. B* **2005**, *109*, 18831–18838.
- (48) Henderson, M. A. Acetone Chemistry on Oxidized and Reduced  $\text{TiO}_2(110)$ . *J. Phys. Chem. B* **2004**, *108*, 18932–18941.
- (49) Henderson, M. A. Effect of Coadsorbed Water on the Photodecomposition of Acetone on  $\text{TiO}_2(110)$ . *J. Catal.* **2008**, *256*, 287–292.
- (50) Zehr, R. T.; Henderson, M. A. Thermal Chemistry and Photochemistry of Hexafluoroacetone on Rutile  $\text{TiO}_2(110)$ . *Phys. Chem. Chem. Phys.* **2010**, *12*, 8084–8091.
- (51) Wilson, D. P.; Sporleder, D.; White, M. G. Final State Distributions of Methyl Photoproducts from the Photooxidation of Acetone on  $\text{TiO}_2(110)$ . *J. Phys. Chem. C* **2012**, *116*, 16541–16552.
- (52) Bogumil, K.; Orphal, J.; Homann, T.; Voigt, S.; Spietz, P.; Fleischmann, O. C.; Vogel, A.; Hartmann, M.; Bovensmann, H.; Frerick, J.; et al. Measurements of Molecular Absorption Spectra with the SCIAMACHY pre-Flight Model: Instrument Characterization and Reference Data for Atmospheric Remote Sensing in the 230–2380 nm Region. *J. Photochem. Photobiol. A: Photochem.* **2003**, *157*, 167–184.
- (53) Guo, Q.; Xu, C.; Ren, Z.; Yang, W.; Ma, Z.; Dai, D.; Minton, T. K.; Yang, X. Methyl Formate Production on  $\text{TiO}_2(110)$ , Initiated by Methanol Photocatalysis at 400 nm. *J. Phys. Chem. C* **2013**, *117*, 5293–5300.